TONAL FAN NOISE OF AN ISOLATED AXIAL FAN ROTOR DUE TO INHOMOGENEOUS COHERENT STRUCTURES AT THE INTAKE

Michael STURM, Thomas CAROLUS

UNIVERSITY OF SIEGEN, Institute for Fluid- and Thermodynamics,
Paul-Bonatz-Strasse 9-11, D-57068 Siegen, GERMANY

SUMMARY

In spite of low circumferential Mach number and no obvious disturbances up- and downstream, the sound of axial fans is often dominated by distinctive tones at blade passing frequency (BPF) and its higher harmonics. Flow visualization at the air intake and a correlation analysis of measured blade pressure fluctuations reveal that quasi-stationary coherent structures exist in the inflow which may act as a source of the tones. They can partly be suppressed by a hemispherical inflow control device which supports this finding.

INTRODUCTION

A typical measured acoustic spectrum of an axial fan is broadband with some tones, most often at blade passing frequency (BPF) and its higher harmonics, Fig. 1. Theoretically, tones at BPF should not occur, when the rotor is completely isolated, i.e. struts and guide vanes are non-existent or very far up- or downstream, the inlet geometry is symmetric and the rotor is rotating at a low characteristic circumferential Mach number. As proven by many authors [1, 2, 3], the unavoidable steady loading as well as the volume displacement by the moving blades is not the source of the BPF sound from low Mach number fans. Presumably, Prandtl [4] was one of the first who observed a correlation between the BPF noise and the condition of the inflow. Hanson [5] investigated a fan rotor in a free environment and found large stretched turbulent eddies by hot-wire measurements entering the rotor plane. Measurements with some pressure transducers on the surface of the blades revealed that disturbances in the clean inflow have the same strength like a defined disturbance of a cylinders placed in front of the rotor. Hanson attributed the large coherent structures to the atmospheric turbulence. Mani [6] developed an analytical model for rotor noise due to incident turbulence. He found that the tones at blade passing frequency vanishes when the ratio between the integral length scale of the incident turbulence and the spacing between the blades is smaller than 0.5. Thus, he showed a relationship between the tonal noise of isolated rotors and incident coherent structures. While investigating a tail rotor of a helicopter, Signor et al. [7] emphasized the influence of turbulence intensity

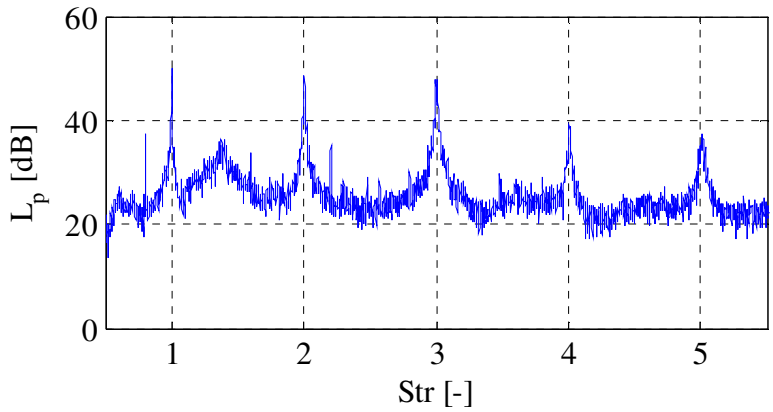

Fig. 1: Time averaged acoustic spectrum of an isolated axial fan rotor with no obvious disturbances up- and downstream

in the incident coherent structures as an important factor regarding the amplitude of the tone at blade passing frequency.

All studies have in common that incident coherent structures are potential sources for tones at blade passing frequency in case of an isolated fan rotor, but no concluding explanation or visualization of these coherent structures exists. The objective of this study is to unveil and characterize coherent flow structures in the inlet of a prototype industrial fan rotor by means of experimental flow visualization and correlation of pressure fluctuations on the rotating blade surfaces.

TEST RIG

To investigate the phenomenon of the BPF noise in a seemingly uniform flow a low pressure axial fan unit, Fig. 2 and Tab.1, was investigated on a standardized measurement test rig, Fig. 3. The impeller has been manufactured and balanced with very high precision to avoid any non-aeroacoustic sound sources. The five cambered and swept blades are designed with an in-house design software for axial fans. To ensure a homogenous inflow a bell mouth type inlet nozzle with a ¼ rotor diameter radius is employed. Thin supporting struts are positioned one rotor diameter downstream of the rotor. No other obstructions are present.

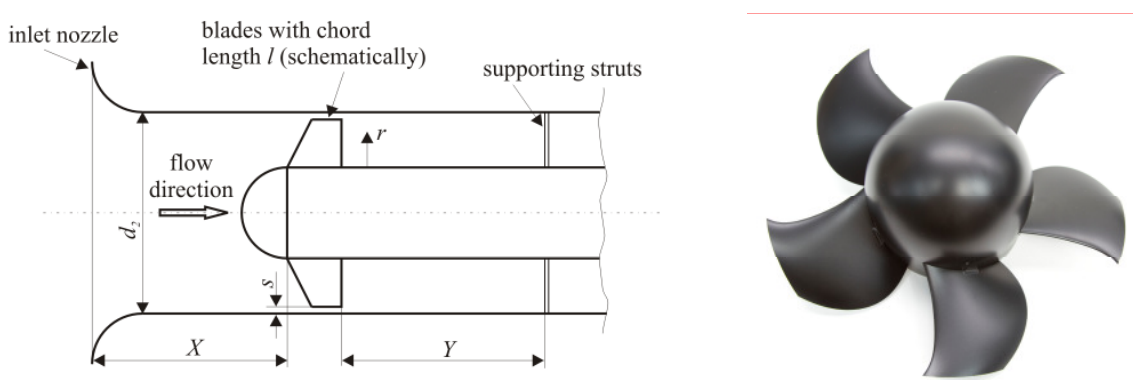

Fig. 2: Axial fan unit investigated (left; to scale; X = 290 mm, Y = 300 mm) and topview of the impeller

Table 1: Important parameters of the impeller

Duct diameter	d_2	0.3 m
Hub diameter	d_1	0.135 m
Rotational speed	n	3000 min^{-1}
Design flow rate	$\dot{V}_{opt}$	0.65 m^3/s
Design flow rate coefficient	$\rho_{opt} = 4 \cdot \dot{V}_{opt} / (\pi^2 \cdot d_2^3 \cdot n)$	0.195
Number of blades	z	5
Tip clearance ratio	s/d_2	0.1 %
Circumferential Ma at d_2	$Ma = \pi \cdot d_2 \cdot n / a$	0.139
Re at d_2	$\text{Re} = \pi \cdot d_2^2 \cdot n / \nu$	$9.36 \cdot 10^5$

The impeller takes the air from a large semi-anechoic room and exhausts into a duct with an anechoic termination. The operating point is controlled by a throttle downstream of the termination. The flow rate is determined by a calibrated hot film probe in the duct. The sound pressure in the anechoic room is measured by three microphones (Brüel & Kjaer type 4190) with a radial distance of 1.3 m and an angular spacing of 35° from the axis of rotation. The sound power radiated into the free field on the suction side of the fan is derived from the sound pressure measured at several positions on a control surface around the inflow. The duct sound power is measured by a microphone downstream of the impeller. In order to compensate for pseudo sound and duct mode effects, the microphone is equipped with a slit tube and a nose cone (as recommended in [8]).

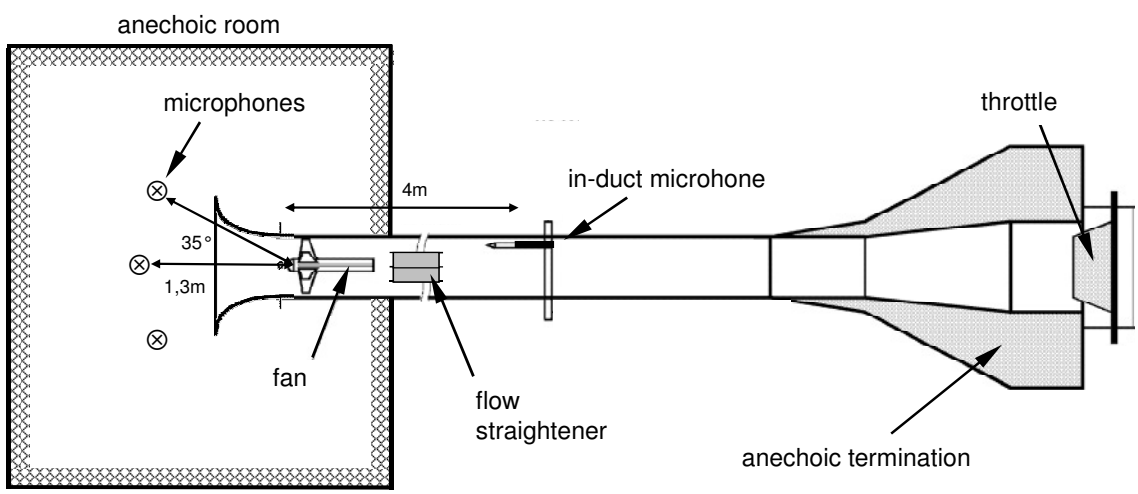

Fig. 3: Test rig (schematically)

Two blades are instrumented with seven flush mounted pressure transducers placed on the suction side, see Fig. 4. The same arrangement of sensors is made for another two blades on the pressure side. The pressure transducers have been calibrated with a white noise excitation signal to consider the whole range of frequencies. A slip ring transducer transfers the signals from the rotating impeller system to the stationary laboratory system. The random noise from the slip ring transducer is

found to be negligible. Due to the blade spacing, pressure signals from pairs of sensors with an angular distance of 144° have been recorded. In addition, the signals from the four microphones indicated in Fig. 3 have been recorded synchronously. Note that the measurements always have been made at a rotational speed of n = 3000 min^{-1} and at the fan design operating point φ_{opt} = 0.195.

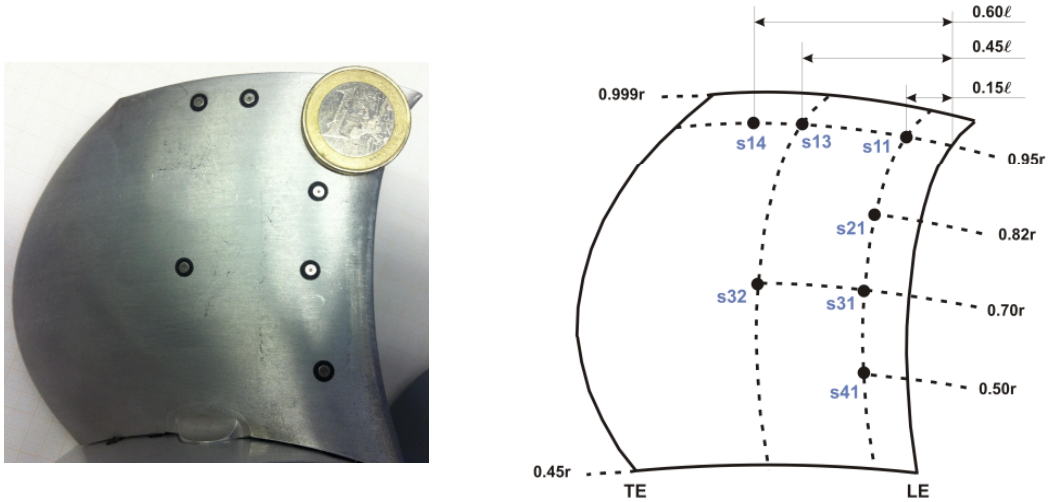

Fig. 4: Suction side of a manufactured blade with miniature pressure transducers (left) and the corresponding locations on the blade (right)

All time signal of the sound pressure or blade pressure were captured with a sampling frequency f_s = 25.6 kHz. The signal analysis is based on the power spectral density which was obtained by the function *pwelch* in MATLAB™ Vers. 7.11. The parameters chosen for *pwelch* were *window = hann(nfft), noverlap = 0, nfft = length(time signal)/30*. The spectra from the windows have been averaged, their final frequency resolution is Δf = 1 Hz. For all levels, the reference pressure is p_0 = $2 \cdot 10^{-5}$ Pa.

An Inflow Control Device (ICD), Fig. 5, has been designed and built to homogenize the natural inflow and hence to vary the inflow conditions [9]. The ICD consists of a combination of a honeycomb structure and a downstream arranged wire mesh. The hemispherical device can be flange mounted to the nozzle of the test rig.

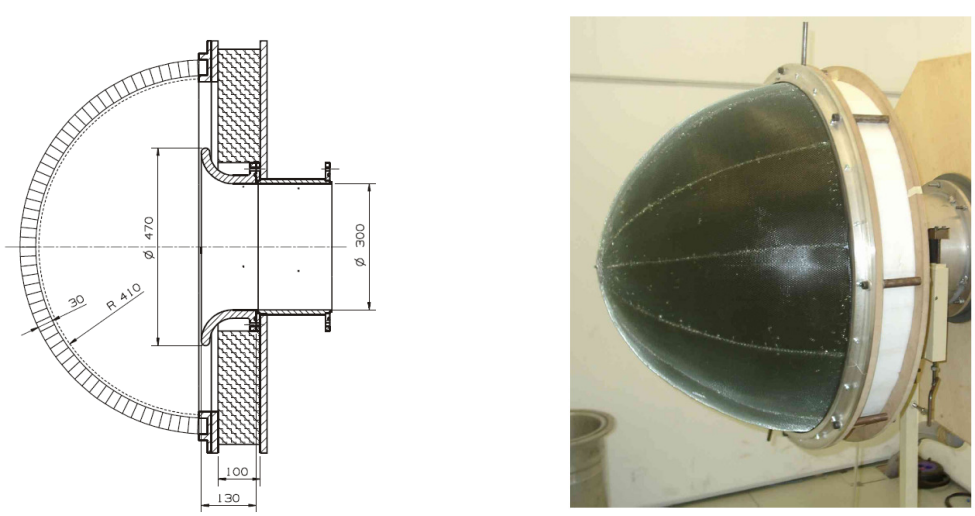

Fig. 5: Inflow Control Device (ICD)

To visualize the flow at the intake of the fan, an array of six horizontal wires has been stretched in front of the nozzle, see Fig. 6. The wires were coated with special oil and heated electrically. A high quality camera was used to record a film of the generated streamlines. To capture a larger area around the intake and not only single streamlines, a smoke generator was also used to produce smoke over a wide region around the intake.

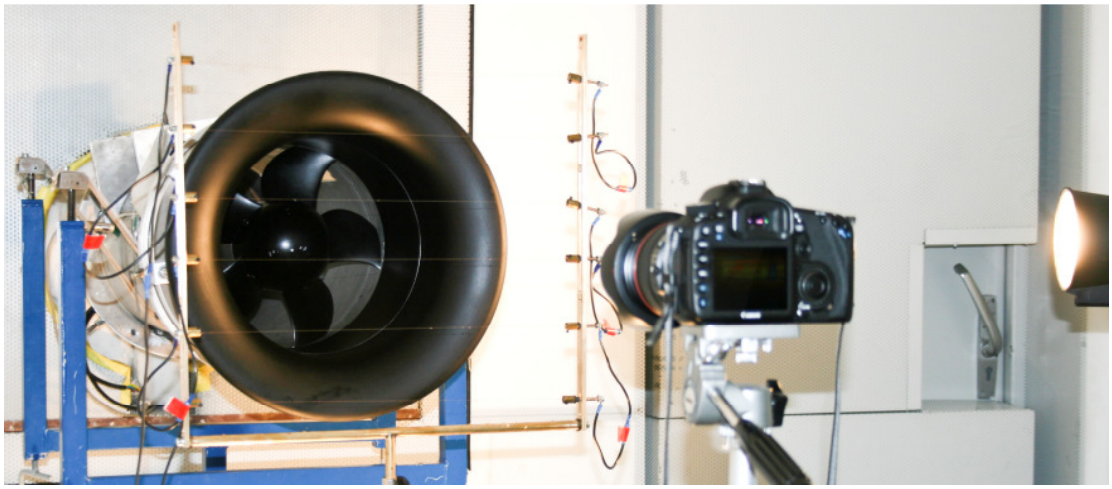

Fig. 6: Experimental set-up for flow visualization at the intake of the fan

SURFACE PRESSURE CORRELATION TECHNIQUE

The sources of BPF tones are periodic pressure fluctuations on the blades of the fan. Possible reasons for those fluctuations are coherent flow structures in the inflow which interact with the rotating impeller blades. To check this hypothesis, a modal analysis is applied to the data from the miniature pressure transducers on the rotating fan blades. Similar data processing has been reported by Bent [10], Tetu [11] and especially Wolfram [12], also applied to tone formation from centrifugal fan impellers.

A mode is thought as a coherent secondary flow structure superimposed by the principal flow pattern associated with blade channel rotating at rotor speed n. Such a mode can be regarded as a wave pattern along the circumference with a finite number of wave peaks in azimuthal direction. If the rotational speed n_{mod} of such an azimuthal mode differs from the rotational speed n of the impeller, interactions occur every time a wave peak hits a blade edge. Because of the rotation those events appear periodically and hence can be the source of periodic fluctuations on the blades.

An azimuthal mode can be characterized by two parameters: The order of the mode m, i.e. the number of wave peaks along the circumference, and the rotational speed n_{mod} of the mode. To calculate these parameters at least two signals $x(t)$ and $y(t)$ of a flow field variable, measured synchronously at a known angular distance θ_{xy}, are required. Here, the time signals of the blade surface pressure are used to perform the analysis. Since modes are highly coherent flow structures, the coherence function (see [13])

$$C_{xy}(f) = \frac{\left|S_{xy}(f)\right|^2}{S_{xx}(f)S_{yy}(f)} \tag{1}$$

is used as an indicator. $S_{xy}(f)$ is the cross power spectral density, and $S_{xx}(f)$, $S_{yy}(f)$ are the power spectral densities of the respective time signals. For frequencies where the coherence is large the phase shift between the two signals is calculated using the relationship for the phase angle

$$\zeta_{xy} = \arctan \frac{\mathrm{Im}\{S_{xy}\}}{\mathrm{Re}\{S_{xy}\}}. \tag{2}$$

Note that the actual phase angle ζ_{xy} may differ from the measured one by an integer multiple of *360* degrees since eq. (2) is bound to *+/- 180* degrees. With that information and the fixed angular distance θ_{xy} of the two sensors, the order of the mode can be calculated using

$$m = \frac{\zeta_{xy}}{\theta_{xy}}. \tag{3}$$

The rotational speed of the mode then becomes

$$n_{\mathrm{mod}} = n - \frac{f}{m} = n\left(1 - \frac{Str \cdot z}{m}\right). \tag{4}$$

In eq. (4), the rotational speed of the impeller n has to be considered since the pressure transducers are rotating with the impeller. Every time a lobe of the mode crosses a blade an interaction occurs. The number of those interactions N_{int} defines the acoustically relevant frequency of mode-blade interactions

$$f_{\mathrm{int}} = N_{\mathrm{int}}\left(n - n_{\mathrm{mod}}\right) \tag{5}$$

or in dimensionless form in terms of a Strouhal number

$$Str_{\mathrm{int}} = \frac{f_{\mathrm{int}}}{n \cdot z}. \tag{6}$$

Interactions occurring simultaneously are considered as one since it is believed that they only affect the level but not the frequency of mode-blade interactions. The actual number of interactions N_{int} is calculated via a simple counting routine for each mode.

Note that with this procedure only modes moving relative to the pressure transducers can be detected but not those rotating with the same rotational speed as the impeller. Since it is believed that the low-frequency BPF noise is induced by low-frequency blade surface pressure patterns the signals of the miniature pressure sensors are analyzed up to a Strouhal number $Str_{max} = 5$.

RESULTS

Evaluating the measured time of the miniature pressure transducers via eqs. (1) and (2) one obtains coherence and phase data as shown in Fig. 7. Ambiguous phase data has been corrected by adding multiples of 360°. The red line shows a straight line with a slope of $\zeta_{xy}/Str = 720$. The jumps of the phase data in some frequency ranges is due to minor inaccuracies of the measurements. However, the slope of the straight line matches the one of the measured phase data perfectly. Combining eqs. (3) and (4) and using the measured slope of the straight line of $\zeta_{xy}/Str = 720$ yields zero for the rotational speed of mode

$$\mathrm{n}_{\mathrm{mod}} = \mathrm{n} \cdot \left(1 - \mathrm{z} \cdot \Theta_{\mathrm{xy}} \cdot \left(\frac{\zeta_{\mathrm{xy}}}{\mathrm{Str}}\right)^{-1}\right).$$

This suggests that some kind of stationary modes exist. But since modes are coherent structures, a second indicator regarding the coherence has to be proofed. The plot of the coherence in Fig.7 shows high peaks at discrete values of *Str* with a decreasing amplitude as *Str* increases. For the following results of the modal analysis the threshold of the coherence function is chosen to be 0.75. This value is taken as indicator for the existence of coherent structures, hence, evaluation of eqs. (3) to (6) is carried out only for the corresponding frequencies.

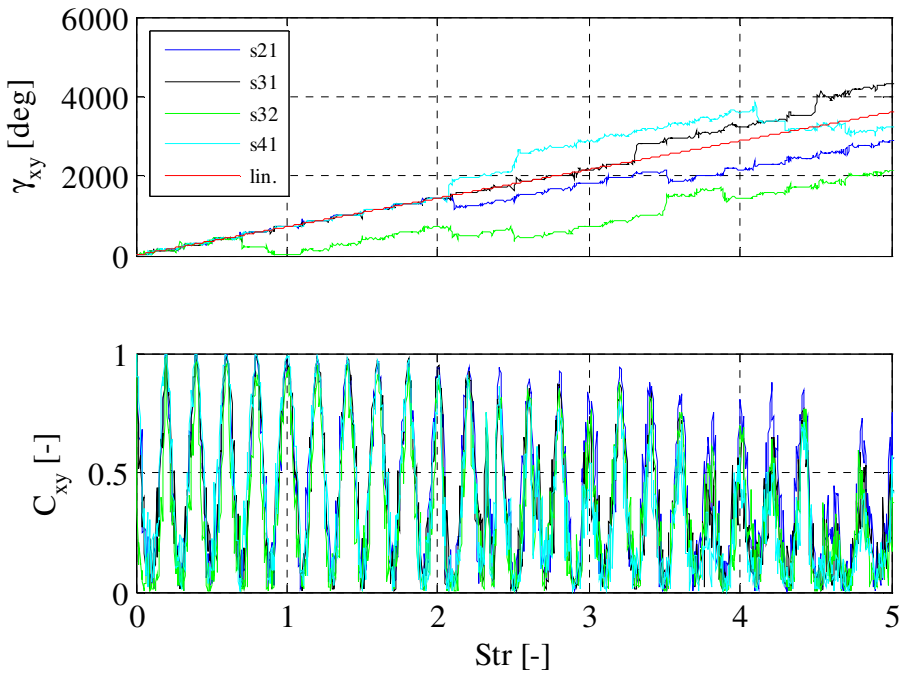

Fig. 7: Phase and coherence data of different pressure sensors

The detected modes with their order and rotational speed are shown in Fig. 8. Modes are existent which are nearly stationary with respect to the laboratory system. It is also obvious that the number of modes and hence the coherence is decreasing in the direction of the hub. Considering that the blades interact with those stationary coherent structures, the azimuthal modes are potential candidates for the source of tonal sound. The frequencies of these tones depend on the number of interactions per revolution between the coherent structures and the rotating blades. In turn, the number of interactions depends on the order of the modes m, the number of blades z and the rotational speed of the modes n_{mod} and that of the fan n. Looking at Fig. 8, one can see that the mode order m is the only variable of these four parameters. Beside the fixed values of z and n, the measurements showing that also $n_{mod} = 0$ for all detected modes. Now, one can determine the number of interactions between the mode and the blades for one revolution via a counting routine to obtain the interaction frequency for each mode. Fig. 9 (bottom) shows how often a specific interaction frequency has been detected for the different modes. For example, a mode order of $m=1$ gives an interaction frequency of $Str_{int} = 1$, as well as a mode order of $m=5$. Only modes that have been detected by all pairs of sensors are taken into account for the calculation of Str_{int}.

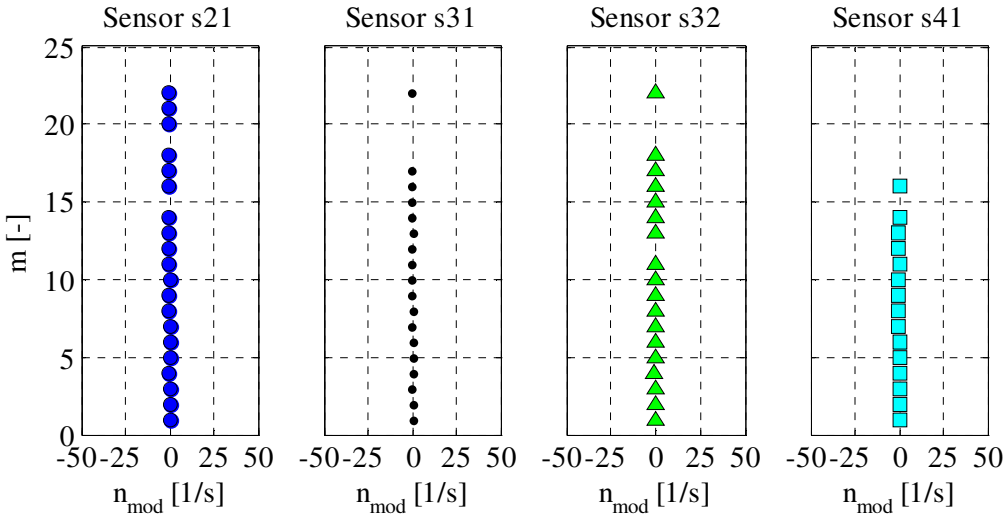

Fig. 8: Detected modes: Mode order as a function of mode rotational speed n_{mod}

Comparing the spectrum of the interaction frequencies with the acoustic spectrum (see Fig. 9, top), one can observe a rather satisfactory correlation (except for *Str = 5)*. The results so far are based on measurements on the suction side of the blades. Although not shown here, similar results have been obtained at the pressure side of the blades.

Unfortunately, the modal analysis is not able to identify any causality, i.e. it does not explain the origin of the modal structures. To get an idea of the source of the modes, Fig. 10 shows the blade pressure fluctuations at various locations on the blade surface. The amplitudes of the pressure fluctuations decrease in streamwise direction (see Figs. 10a and b), which indicates that the coherent structures dominate at the leading edge where the flow approaches the blade initially. Furthermore, the fluctuations seem to be higher on the suction side in the leading edge region of the blade (see Fig. 10c), while they reach the same level on the pressure side in the center of blades (see Fig. 10d). Although not shown here, there is no variation of the level of pressure fluctuations in radial direction. All these results are indicators that the detected azimuthal modes origin from the inflow.

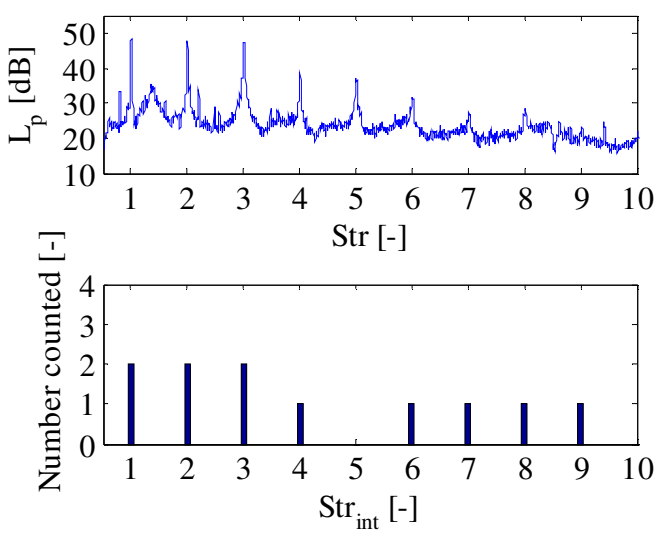

Fig. 9: Comparison of the acoustic spectrum (top) and the number of detected interaction frequencies (bottom)

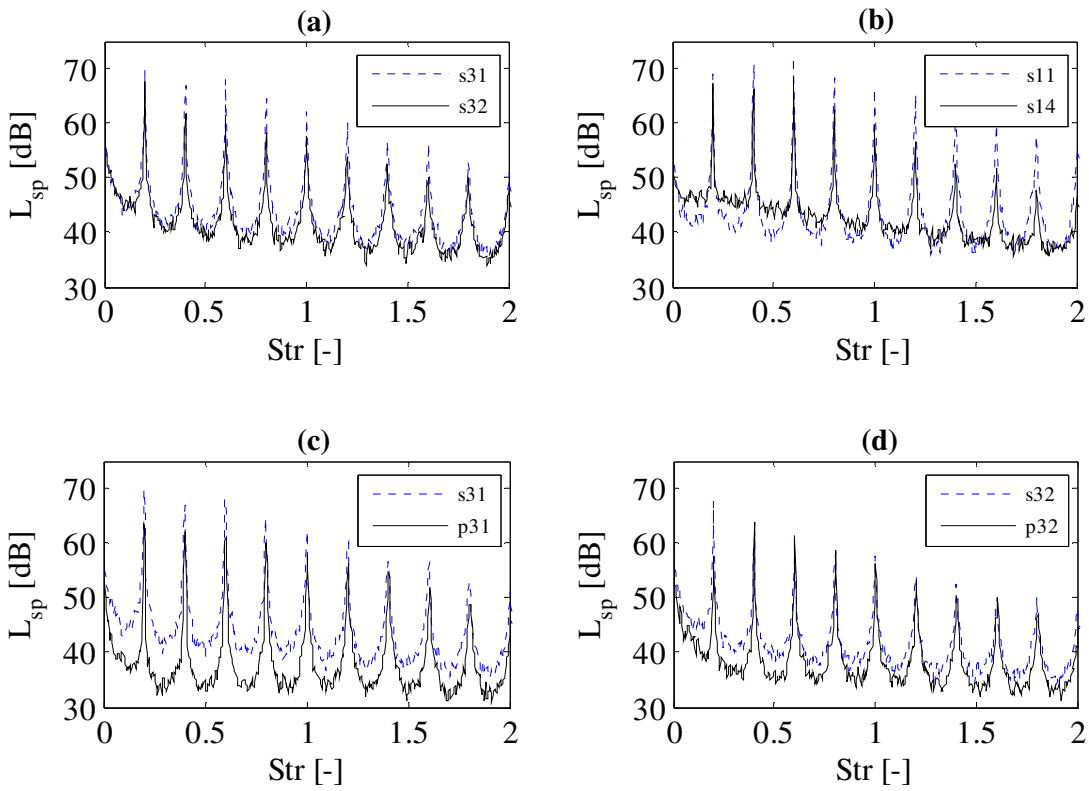

Fig. 10: Comparison of the acoustic spectrum (top) and the number of detected interaction frequencies (bottom)

In a second series of experiment the inlet control device (ICD) was used in front of the bell mouth inlet. The results are shown in Fig. 11. With ICD the pressure fluctuations show a significant reduction as compared to the natural inflow (Fig. 11 left). Both, tonal and broadband components are clearly reduced. Only the first peak at shaft speed (*Str* = 0.2) is affected very little. The acoustic spectrum (Fig. 11 right) reflects these findings to a certain degree. The tone at BPF is reduced considerably (but not completely eliminated), whereas higher harmonics nearly vanish. The broadband sound components seemingly are not affected by the ICD. At least, this confirms once more that the sources of the BPF-related tones are closely linked to coherent structures in the inflow.

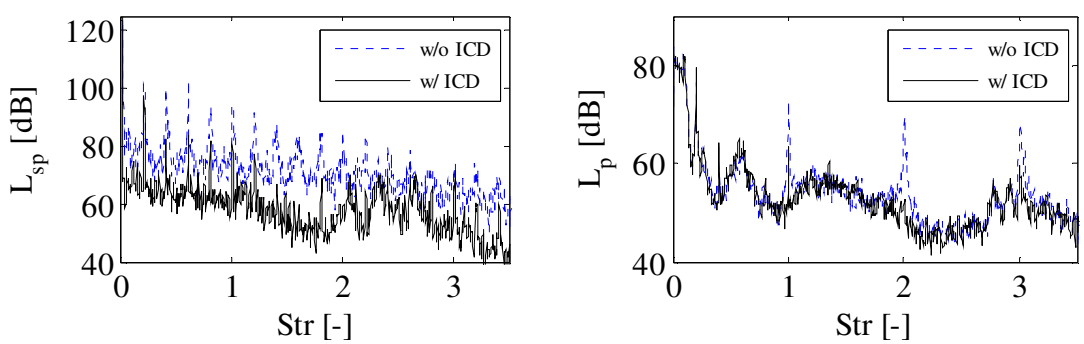

Fig. 11: Typical effect of inlet turbulence control device (ICD); left: blade surface pressure (sensor s32), right: acoustic spectrum

In order to further verify this hypothesis, the flow at the bell mouth inlet has been visualized by smoke. Fig. 12 depicts snapshots at arbitrary time instances with arbitrary distributed smoke (left) and controlled defined streamlines of smoke (right). Helical streamlines indicate vortex type struc-

tures. Closer observation shows that circumferential and radial position as well as core diameter of these structures varies with time. However, closer observation proves that the characteristic time scale of this variation is very small as compared to the rotational speed of the impeller, i.e. the coherent structures are quasi-stationary for many revolutions of the impeller. Thus the fan blades cut through the coherent structure several times which explains the periodic force fluctuations on the blades observed. These coherent structures are self-induced, since no obstruction or asymmetry of inlet is present. Hence, obviously a natural "clean" inflow does not necessarily correspond to the common assumption of a uniform, undisturbed inflow.

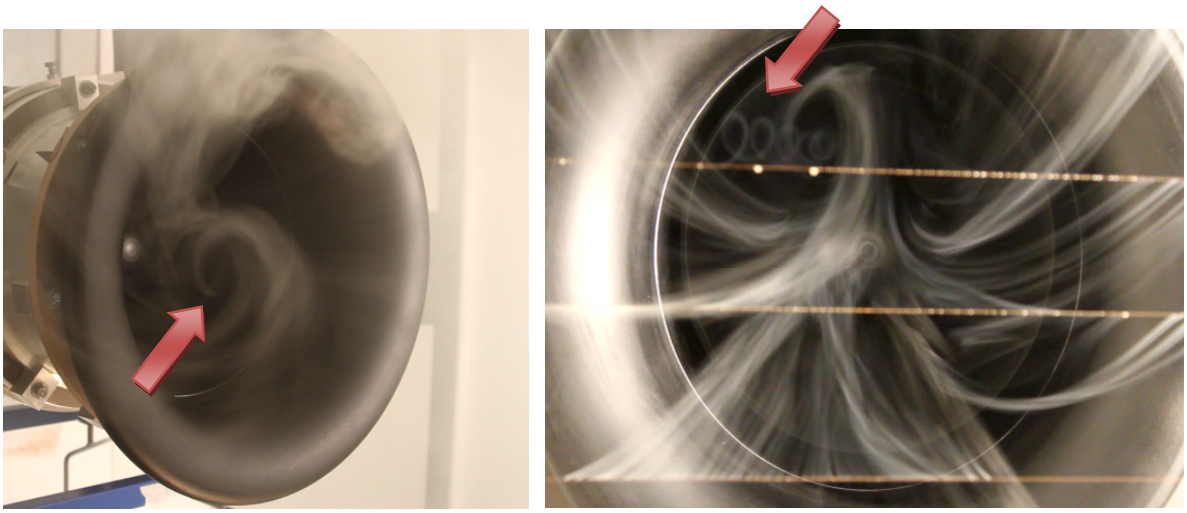

Fig. 12: Inflow: Flow visualizations at different instances of time

SUMMARY AND CONCLUSIONS

The flow at the intake of axial fans is often treated as uniform and purely axial. With this assumption and no other disturbances from up- or downstream obstructions present no tones at BPF and higher harmonics should be produced. This is in contrast to many experiments. In this study a correlation analysis has shown that (i) coherent structures in the fan inlet exist; (ii) these structures are quasi-stationary with respect to the laboratory system; (iii) they presumably are self induced in the inlet region. Measurements with an inflow control device that homogenizes the inflow support the latter conclusion, since blade surface pressure fluctuations and tone production clearly can be reduced. Flow visualization with smoke reveals stretched helical vortices entering the fan impeller. The fact that almost every mode order from 1 to 20 exists suggest that a field of vortices is entering the fan simultaneously. The quasi-stationary character of the vortex field corresponds to the stationary modes as predicted by the blade pressure correlation technique. The interaction of this non-homogeneous flow at the inlet and the blades cause the periodic force fluctuations on the blades and hence BPF-related tones. The study so far gives no explanation on the self-induction mechanism. It would be helpful to perform a transient numerical flow field simulation. To capture the vortex formation mechanisms at the intake the computational domain needs to include the fan with the complete anechoic room indicated in Fig. 3. This makes the computation rather complex and expensive. On top of that further effort is required to link the blade surface pressure fluctuations qualitatively to the acoustics.

NOMENCLATURE

a	[m/s]	speed of sound
BPF	[Hz]	blade passing frequency
C_{xy}	[-]	coherence function
d_2	[m]	duct diameter
f	[Hz]	frequency
f_{int}	[Hz]	interaction frequency
Δf	[Hz]	frequency resolution
f_s	[Hz]	sampling rate
ICD	[-]	Inflow Control Device
l	[m]	chord length
LE	[-]	leading edge
L_p	[dB]	level of acoustic pressure
L_{sp}	[dB]	level of surface pressure
m	[-]	mode order
Ma	[-]	circumferential Mach number
n	[min^{-1}]	rotational speed
n_{mod}	[min^{-1}]	rotational speed of mode
N_{int}	[-]	number of interaction
p_0	[Pa]	reference pressure
r	[m]	impeller radius
Re	[-]	Reynolds number
s	[m]	tip clearance
S_{xx}	[Pa^2/Hz]	power spectral density
S_{xy}	[Pa^2/Hz]	cross power spectral density
Str	[-]	Strouhal number
Str_{int}	[-]	interaction Strouhal number
TE	[-]	trailing edge
z	[-]	number of blades
ζ_{xy}	[deg]	phase angle
Θ_{xy}	[deg]	angular spacing between sensors
λ	[-]	hub/tip ratio
ν	[m^2/s]	kinematic viscosity
φ	[-]	flow rate coefficient

ACKNOWLEDGMENTS

This investigation is funded by the “Deutsche Forschungsgemeinschaft (DFG)”. The authors gratefully acknowledge this support.

BIBLIOGRAPHY

[1] M. E. Goldstein – *Aeroacoustics.* McGraw-Hill, USA, **1974**

[2] M. Roger – *Noise in Turbomachines – Noise from moving surfaces*. VKI-Lecture Series 2000-02, von Karman Institute for Fluid Dynamics, Belgium, **2000**

[3] S.-J. Zhu, X.-J. Wu – *Research on the farfield tonal fan noise at small mach number*. Proceedings of ASME International Mechanical Engineering Congress and Exposition, Chicago, Illinois, USA, **2006**

[4] L. Prandtl – *Remarks on aircraft noise (In German).* Zeitschrift für technische Physik, Vol. 2, pp. 244-245, **1921**

[5] R. Mani – *Noise due to interaction of inlet disturbances with isolated stators and rotors*. Journal of Sound and Vibration, Vol. 17, No. 2, pp. 251-260, **1971**

[6] D.B. Hanson – *Spectrum of rotor noise caused by atmospheric turbulence.* J. Acoust. Soc. Am., Vol. 56, No. 1, pp. 110-126, **1974**

[7] D. B. Signor, G. K. Yamauchi, M. Mosher, M. J. Hagen, A. R. George – *Effects of ingested atmospheric turbulence on measured tail rotor acoustics.* Journal of the American Helicopter Society, Vol. 41, No. 1, pp. 77-90, **1996**

[8] International Organization for Standardization – *Acoustics – Determination of sound power radiated into a duct by fans and other air-moving devices – In-duct method*. International Organization for Standardization, Switzerland, **2003**

[9] M. Schneider – *Der Einfluss der Zuströmbedingungen auf das breitbandige Geräusch eines Axialventilators*. Vol. Nr. 478 of Fortschritt-Berichte VDI Reihe 7: Strömungstechnik, Ph. D. Dissertation, VDI-Verlag GmbH, Düsseldorf, **2006**

[10] P. H. Bent – *Experiments on the aerodynamic generation of noise in centrifugal turbomachinery*. PhD Thesis, Pennsylvania State University, **1993**

[11] L. G. Tetu – *Experiments on the aeroacoustics of centrifugal turbomachinery*. M.Sc. Thesis, Pennsylvania State University, **1993**

[12] D. Wolfram, T. Carolus – *Experimental and numerical investigation of the unsteady flow field and tone generation in an isolated centrifugal fan impeller*. Journal of Sound and Vibration, Vol. 329, pp. 4380-4397, **2010**

[13] J. S. Bendat, A. G. Piersol – *Random Data – Analysis and measurement procedures*. John Wiley & Sons, Inc, 4th Edition, **2010**

© M. Sturm, Th. Carolus